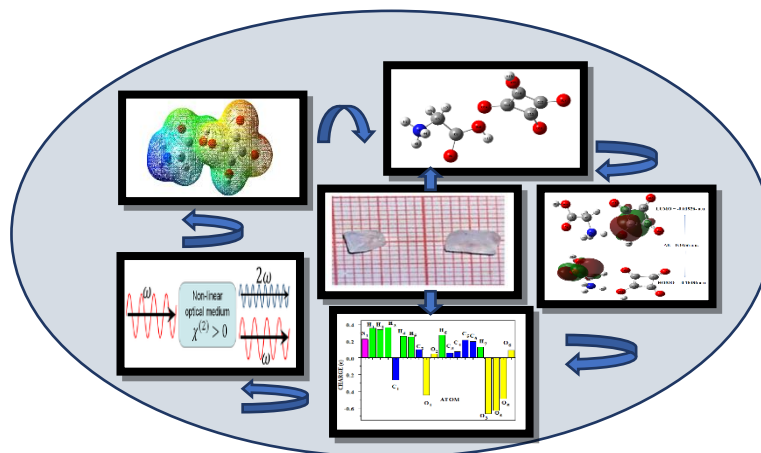


Crystal Structure, Vibrational Spectroscopic, Electronic Properties And DFT Calculations Of L-Glycinium Hydrogen Squarate: A Non-Linear Optical Single Crystal

S. Arulmani¹, K. Deepa², E. Chinnasamy³, M. Victor Antony Raj⁴, J. Madhavan⁴ and S. Senthil^{1,*}

Graphical abstract



Abstract: Good quality and optically transparent L-glycinium hydrogen squarate (GSQ) single crystal as grown from its aqueous solution by slow solvent evaporation technique at room temperature method. The Single X-ray Diffraction (SXRD) analysis shows that the GSQ compound crystallized in monoclinic crystal system with non-centrosymmetric P21/n space group. FT-IR investigation helps to detect the discrete functional groups existing in the GSQ single crystal. The optimized structure and molecular geometry of the GSQ single crystal has been analysed by the density functional theory (DFT) method with B3LYP/6-311++G (d, p) basis set. HOMO- LUMO energy gap value. The second order nonlinear optical (NLO) behaviour of GSQ single crystals has been evaluated by Kurtz-Perry powder techniques. UV-Visible study was performed to analyse the optical transparency by identifying the cut-off wavelength and it is found to be 286 nm for the grown crystal. From, the dielectric studies it is observed that both dielectric constant and dielectric loss of the sample decrease with increase in frequency and it was carried out in the high frequency range (1–7 MHz).

Key words: Crystal growth, DFT, Dielectric studies, FT-IR, Homo-Lumo , UV- Vis, NLO,.

1. INTRODUCTION

In past few decades, abundant researchers has been focused on the development of new non-linear optical (NLO) materials because of their vital applications in the fields such as generation of higher harmonic frequencies, frequency mixing, telecommunication, electro-optic modulation, optical disk data storage device, optical parametric oscillator, optical disk data storage device [1] etc.,. Basically, the nonlinear optical materials (NLO) are expected to own enormous nonlinear optical coefficients,

suitable transparency and phase matchable properties. In Organic molecules, owing to their molecular flexibility it also exhibits to improve the NLO properties in an effective manner than the inorganic molecules. Organic single crystal possesses the potential advantages than the inorganic materials in NLO applications, including higher hyperpolarizability [2]. In general, the heterocyclic compounds containing a nitrogen ring, this nitrogen ring can be acts as the proton acceptor of the molecule [3] and the organic compounds with carboxylic or phenolic groups can be act as the donor one. Its helps to develop the donor-acceptor molecule in a system. The polarizable nature of hydrogen atom occurs due to the formation of a strong hydrogen bonds. This formation as covalently bonded to partially positive charged nitrogen atom and it will be interacting with a partially negative charged oxygen atom leading to increases the molecular hyperpolarizability of the compound [4]. The Proton transfer will be occurred due to the formation of strong hydrogen bonding of the compound, these proton transfer helps to rise the interesting properties such as optical applications and non-linear optical behaviour of the materials [5]. The crystalline proton

- ¹Department of Physics, Government Arts College for Men, Nandanam, Chennai, India
- ²Department of Chemistry, Government Girls Hr. Sec. School, Poonamallee, Chennai, India
- ³Department of Physics, St. Joseph's Arts College, Kovur, Chennai, India
- ⁴ Department of Physics, Loyola College, Chennai, India
- Corresponding author: ssatoms@yahoo.co.in

transfer compounds play a vital role in laser technology, optical communications, optoelectronic process, optical signal processing, photo catalyst, as well as the biological applications [6,7]. Organic single crystals with the required conjugated electrons are the attractive candidates, because it has the huge nonlinear optical coefficients [8]. In the present work, the crystal structure, spectroscopic analysis and Theoretical investigation have been carried out for the title compound of L-Glycinium hydrogen squarate (GSQ) and their results are discussed. Further, optimized structure, spectral measurements, thermodynamic properties and hyperpolarizability also calculated by using density functional theory (DFT) [9]. The dielectric behaviour, optical properties and second order efficiency of the GSQ single crystal were investigated.

2. EXPERIMENTAL APPROACHES

2.1 Synthesis

L-Glycine – $C_6H_{14}N_4O_2$ (Sigma–Aldrich, 99%) and Squaric acid ($C_4H_6O_6$) (Sigma–Aldrich, 99%) were taken in equimolar ratio (1:1). The Glycinium hydrogen Squarate (GSQ) single crystals has been grown by the method of slow evaporation process at room temperature. The solution was mixed together until to attain the supersaturated level and the solution was filtered, decanted into a 150 mL beaker and sealed with silver foil paper, then the beaker was housed for slow evaporation method in a dust free atmosphere. The GSQ single crystal was harvested within 35-40 days from the mother solution. The photograph of GSQ single crystal is shown in fig.1. The Crystal data and full structure refinement details of grown single crystal has been shown in table 1.

TABLE-1

Crystal data and structure refinement details of GSQ single crystal

Chemical formula	$C_6H_7NO_6$
Formula weight	189.13
Crystal system	Monoclinic
Space group	$P2_1/n$
Temperature (K)	293(2) K
a	$a = 7.26500(10) \text{ \AA}$
b	$b = 21.9009(3) \text{ \AA}$
c	$c = 10.0170(5) \text{ \AA}$
α	$\alpha = 90^\circ$
β	$\beta = 95.430(2)^\circ$
γ	$\gamma = 90^\circ$
V	$1586.65(9) \text{ \AA}^3$
Z	8
Absorption coefficient	0.145 mm^{-1}
Crystal size (mm)	$0.300 \times 0.250 \times 0.200 \text{ mm}^3$
Diffractometer	Bruker AXS Kappa APEX2 CCD Diffractometer
No. of parameters	403
No. of restraints	5
Refinement method	Full-matrix least-squares on F ²
Goodness-of-fit on F ²	1.178
Final R indices [I > 2 σ (I)]	R1 = 0.0656, wR2 = 0.2093
R indices (all data)	R1 = 0.0714, wR2 = 0.2144
Absolute structure parameter	-0.4 (9)
Largest diff. peak and hole	0.370 and -0.360 $e \cdot \text{\AA}^{-3}$



Fig. 1. Photograph of as grown GSQ single crystal.

3.1 Computational details

The optimized structural characteristics and the normal vibrational modes of Glycinium hydrogen squarate (GSQ) molecule were studied by using Density Functional Theory (DFT) calculations. The original molecular geometry of the L-glycinium hydrogen squarate (GSQ) single crystal was taken from the Crystallographic Information File (CIF) obtained from the single crystal XRD structure analysis. Based on this optimized structure, the vibrational frequencies of the molecules and their intensities also calculated. All the calculated vibrational modes of the molecules are positive and this report shows that the structures are stable. In addition, the HOMO-LUMO energy gap of the molecules, nonlinear optical properties of the materials, and other physical properties of the GSQ single crystal were investigated by using the optimized structures and the vibrational modes of the compound.

3.2 Optimized Geometry

The optimized structural parameters of L-Glycinium Hydrogen Squarate (GSQ) single crystal were calculated B3LYP levels with the 6–311++G (d, p) basis set and the values are recorded in Table 3. The calculated structure of the molecule and the atom-labeling scheme adopted for the calculation are shown in Fig.2. The GSQ molecule has five C-C bonds, one C-N bonds, two C-H bonds, two H-O, three N-H bonds and six C-O bond, one O-O bond. The enormously close similarity has been observed between the geometrically optimized structure of the GSQ compound and the actual crystal structure of this molecule [10,11]. The regular distances between the bond of C-C and C-O calculated by DFT method with B3LYP/6–311++G (d, p) basis sets are 1.3424 Å and 1.3997Å, respectively. The oxygen atoms are bonded to the carbon atoms form the square shape of the molecule. The replacement of squaric acid, a large attraction is applied on the valence electron cloud of the carbon atom. From these, the ring of oxygen atoms resulting to augment the C-H force constant and in turns to decrease the bond length of the atom in a molecule. The C-O bond length shows a comparatively higher value (1.515 Å) due to repulsion between the lone pair of an electron on the oxygen atom and electron on the carbon atom in the ring. In GSQ single crystal, the bond angle of O6-C6-C5 = 139.5° is larger than the bond angle of O1–C2–O2 = 120.0. The Variation of the bond angles has been described on the basis of Valence shell electron pair

repulsion theory. The values of selected bond length and bond length as shown in Table 2. It was nearly coincided with the experimental value.

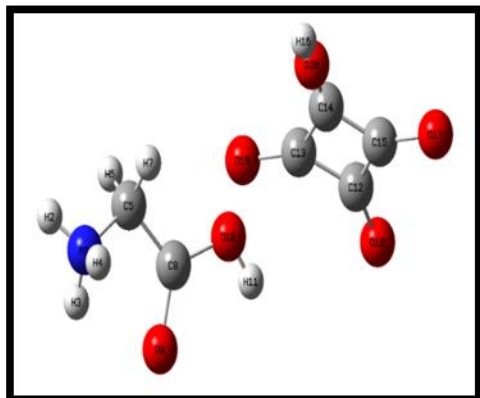


Fig. 2. Optimised molecular structure of glycinium hydrogen squarate

TABLE-2:

The inter-atomic parameters of GSQ molecule compared with observed and calculated values.
Selected bond length (Å)

ATOMS	OBSERVED BOND LENGTH	CALCULATED BOND LENGTH
C(1) - O(1)	1.255	1.321
C(1) - C(2)	1.441	1.396
C(1) - C(2)	1.480	1.423
C(1) - C(4)	1.316	1.296
C(2) - O(2)	1.465	1.411
C(2) - C(3)	1.238	1.201
C(3) - O(3)	1.503	1.492
C(3) - C(4)	1.251	1.232
C(4) - O(4)	1.317	1.302
C(5) - O(5)	1.437	1.421
C(5) - C(6)	1.460	1.452
C(5) - C(8)	1.254	1.240
C(6) - O(6)	1.480	1.395
C(6) - C(7)	1.255	1.246
C(7) - O(7)	1.498	1.435
C(7) - C(8)	1.244	1.232
C(8) - O(8)	1.211	1.201
C(9) - O(9)	1.316	1.312
C(9) - O(10)	1.515	1.520
C(9) - C(10)	1.485	1.482
C(10) - N(1)	1.2821	1.2121

Selected bond angle (°)

ATOMS	OBSERVED BOND ANGLE	CALCULATED BOND ANGLE
O(1)-C(1)-C(2)	136.7	139.4
O(1)-C(1)-C(4)	133.9	132.5
C(2)-C(1)-C(4)	89.4	88.4
O(2)-C(2)-C(1)	130.4	131.5
O(2)-C(2)-C(3)	136.6	135.4
C(1)-C(2)-C(3)	93.0	95.5
O(3)-C(3)-C(2)	137.6	137.2
O(3)-C(3)-C(4)	134.7	133.2
C(2)-C(3)-C(4)	87.6	88.6
O(4)-C(4)-C(1)	133.2	135.8

O(4)-C(4)-C(3)	136.9	138.4
C(1)-C(4)-C(3)	89.9	90.1
O(5)-C(5)-C(6)	130.9	130.5
O(5)-C(5)-C(8)	135.7	134.8
C(6)-C(5)-C(8)	93.3	92.4
O(6)-C(6)-C(5)	138.1	139.5
O(6)-C(6)-C(7)	132.9	131.6
C(5)-C(6)-C(7)	89.1	88.4
O(1)-C(2)-O(3)	120.4	120.0

3.3 HOMO-LUMO energy gap

The investigation of the wave function specifies that the electron captivation corresponds to the transition from the ground state to the first excited state. The frontier molecular orbitals investigation is the promising techniques to found the molecular interaction between the molecule. The HOMO value can be act as an electron donor and the LUMO value can be act as electron acceptor respectively. From, the previous explanation the HOMO energy is directly connected to ionisation potential energy and the LUMO energy is directly connected to electron affinity. The eigenvalue of HOMO and LUMO and their energy gap reflect the chemical activity of the molecule. The calculated energies of GSQ molecules are $E_{\text{HOMO}} = -0.18486$ a.u., $E_{\text{LUMO}} = -0.01926$ a.u. and $\Delta E = \text{HOMO-LUMO} = 0.1656$ a.u. is shown in fig. 3. The obtained energy gap values between HOMO and LUMO was very low which indicates that the GSQ single crystal is suitable to the field of Nonlinear optical (NLO) [12].

HOMO energy; $E_{\text{HOMO}} = -0.18486$ eV
LUMO energy; $E_{\text{LUMO}} = -0.01926$ eV
HOMO-LUMO energy gap [13-16],
 $\Delta E_{\text{gap}} = E_{\text{HOMO}} - E_{\text{LUMO}} = 0.1656$

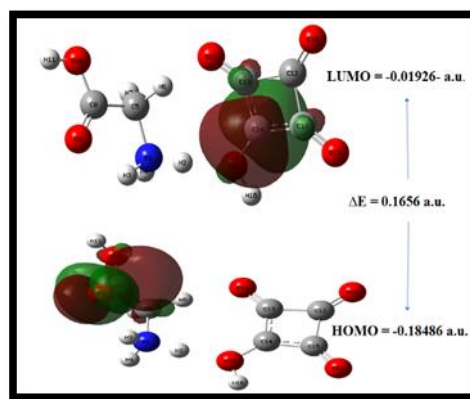


Fig. 3. HOMO – LUMO plot of GSQ crystal

3.4 Spectroscopic Analyses

The enrolled frequency of FT-IR spectral assignments was achieved based on the theoretically predicted wavenumbers by density functional theory (DFT). The vibrational spectra of GSQ single crystal have been studied by applying Density Functional Theory (DFT) with B3LYP/6-311++G (d,p) basis set using gauss view respectively. The experimentally perceived and theoretically computed frequencies of IR intensities and their various vibrational assignments of GSQ single crystal were recorded in Table

3 and spectral assignment graph are displayed in Fig. 4 & 5. The thorough investigation of vibrational assignments of different functional groups were identified in the GSQ single crystal and detailed explanations are given here. The potential energy distribution (PED) of the vibrational modes of GSQ single crystal was also listed clearly in Table 3.

O-H Vibration

The stretching vibrational modes of O-H group have been detected at the value of 2982cm^{-1} [17]. The presence of O-H stretching vibrational mode occurs in the frequency range of 3200cm^{-1} and it was considered as a strong band. In General, the frequency range of $1440 - 1214\text{cm}^{-1}$ [18], has been consider as the Hydroxyl in-plane bending mode of vibration. The in-plane bending mode of hydroxyl group occur in the frequency range of 1372cm^{-1} . The presence of O-H out-plane bending vibrational mode has been allotted in a powerful region it was observed at range of $700 - 600\text{cm}^{-1}$ [19]. The out-plane bending vibrational mode of hydroxyl group are well agreed with the corresponding wavenumber of 609cm^{-1} respectively. The superimposed FT-IR vibration has been perceived at nearly 2713cm^{-1} in the GSQ compound.

N-H Vibration

The heterocyclic compounds have been perceived in the frequency range of $3500-3000\text{cm}^{-1}$ [20]. These values have been considered as N-H stretching vibrational mode. A weaker although sharper band than that of the alcohol (O-H) which is also present in the same region is detected. The NH_2^+ in-plane deformation has been observed at 1639cm^{-1} . Generally, the N-H asymmetric deformation vibrations were perceived in the frequency range of $1760 - 1610\text{cm}^{-1}$ and the symmetric deformations will be appeared in the vibrational range of $1560 - 1485\text{cm}^{-1}$ [21]. N-H symmetric deformation is appeared at the frequency range of 1557cm^{-1} in IR.

C-C Vibration

The stretching vibrational mode of (C-C bond) are expected within the region of $1350-1000\text{cm}^{-1}$ [22-24]. In the present study, the bands which are of different intensities were observed at 1105 , 1121 and 1214cm^{-1} in the FT-IR spectrum. The presence of aromatic compound and hetero aromatic compounds are allocated to the carbon modes of vibrations and it was perceived at the frequency range between 1400 and 1650cm^{-1} [25]. All the C-C band are occurring within the expected range, which indicates that the C-C vibrations are not altered by the presence of the substitution groups. The in-plane vibration of C-C bond is predicted below the range of 1000cm^{-1} . The in-plane vibrations are found at 1105 , 887 , 609 and 754cm^{-1} . The observed vibrations are in the expected region and they are not affected by any other vibration modes.

C-H Vibration

In the presence of aromatic compounds, C-H stretching vibrational modes will be seemed in the range between $3000-3100\text{cm}^{-1}$ [26-30]. The C-H bending and stretching vibrational regions are of the most difficult vibrational regions to interpret in infrared (IR) spectra. The IR band at 2757cm^{-1} has been consider as C-H asymmetric stretching vibration is perceived as a weak IR band. The vibrations of

CH_2 -twist are observed in the frequency range of $1214 - 1021\text{cm}^{-1}$ and CH_2 -rock vibrations has been existed in the frequency region of $1160 - 887\text{cm}^{-1}$ [31]. CH_2 twisting mode is existed in infrared spectra at 1105cm^{-1} as a poor band and CH_2 rocking vibrational mode is existed in the range of 1021cm^{-1} . CH_2 wag vibrational mode is supposed to extend over a broad band frequency in the range of ($1372 - 1214\text{cm}^{-1}$) [34]. CH in-plane bending and CH out-plane bending are perceived between the frequency range of $1300 - 1000\text{cm}^{-1}$ and $887 - 609\text{cm}^{-1}$ respectively [32].

C-N Vibration

The mixing of several modes is possible in the region makes the documentation of C-N bonds very difficult. The frequency range between $1300\text{cm}^{-1} - 1500\text{cm}^{-1}$ indicates the presence of C-N bonds in the GSQ compounds [33]. The vibration bands of the GSQ compound has been perceived at the values of 1080 , 1056 , 966 and 881cm^{-1} in the FT-IR region. Correspondingly, the in plane and out-of-plane bending vibrational mode are occurred below the frequency range of 491cm^{-1} and 752cm^{-1} . The C-N bond was perceived at 1080 , 1056 , 966 and 881cm^{-1} in the FT-IR region.

C-O Vibration

The carbonyl group expressed the strong absorption band for C-O stretching vibrations. This vibration has been perceived region of $1850-1550\text{cm}^{-1}$ [34]. The recorded spectrum shows a sufficient strong band in FT-IR spectrum at the values of 1202cm^{-1} and at 824cm^{-1} in FT-Raman spectrum respectively

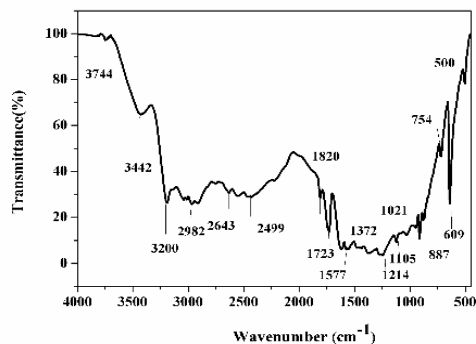


Fig. 4. Experimental FTIR spectrum of GSQ crystal

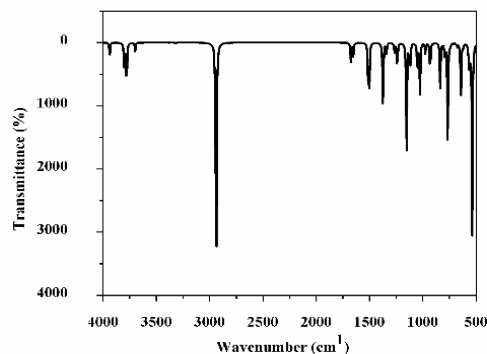


Fig. 5. Theoretical FTIR spectrum of GSQ crystal

TABLE-3:
Observed and calculated frequencies (cm^{-1}) of GSQ

Experimental Frequency (cm^{-1})	Theoretical Frequency (cm^{-1})		IR intensity (KM/Mole)	Force constant (mDyne/A°)	Reduced mass (amu)	% Potential Energy Distribution (PED)
	unscaled	scaled				
-	3938	3781	66.1985	9.7690	1.0687	ν OH (100)
3825	3801	3649	161.5319	9.2932	1.0917	ν NH (97)
3744	3779	3628	246.2390	9.1702	1.0895	ν NH (95)
3442	3699	3551	39.2270	8.3021	1.0297	ν NH (97)
-	3378	3243	0.8916	7.4541	1.1081	ν CH (99)
3200	3318	3185	4.6379	6.8588	1.0573	ν CH (99)
2982	2938	2823	1391.9170	51.7389	10.1677	ν OC (95)
1820	1675	1610	86.7342	1.7201	1.0397	β HNH (66)
1723	1652	1587	97.5900	1.6795	1.0445	$\square\square\square\square$ CC (24)
1577	1513	1453	155.5858	1.5064	1.1160	β HNH (27) + β HCH (43) + $\square\square\square$ HCCO (18)
1484	1503	1444	290.2620	1.4425	1.0826	β HCH (16)
1419	1376	1322	96.1983	2.8498	2.5512	ν CC (25) + β HCH (17) + $\square\square\square$ HCCO (13)
1372	1373	1319	243.4601	2.5188	2.2675	ν CC (31) + β HCH (11)
-	1340	1288	47.4283	1.2938	1.2216	β HCC (24) + $\square\square\square\square$ CC (14) + $\square\square\square\square$ CC O (12) + $\square\square\square\square$ CC O (33)
-	1265	1216	56.3425	2.7753	2.9422	ν CC (26) + β HOO (13) + β CCN (12) + $\square\square\square\square$ CC (12)
1214	1239	1191	131.1267	10.1536	11.2195	ν CC (58)
-	1152	1107	537.2616	8.4140	10.7558	β CCC (5)
-	1126	1082	72.4576	2.4916	3.3298	ν NC (43) + β HCC (13)
1105	1116	1072	90.2713	1.5097	2.0564	ν NC (21) + β HCC (30) + $\square\square\square$ CCO (10)
-	1049	1008	175.2841	1.2384	1.9090	β HNH (11)
1121	1026	985	259.8937	6.8880	11.0971	ν CC (62)
-	974	936	54.2952	6.1474	10.9883	ν CC (24) + β CCC (43)
887	930	893	162.3489	1.2262	2.4027	ν CC (12) + ν OO (13) + $\square\square\square$ CC (14)
-	835	802	210.4687	2.1220	5.1592	ν OO (56)
-	800	769	7.3534	4.6358	12.2801	$\square\square$ CCCC (11) + $\square\square$ OCCC (43)
-	790	759	84.6076	0.7367	1.9984	ν CC (13) + $\square\square$ OCCC (11)
754	765	735	456.4595	3.3486	9.7049	β COO (30)
-	740	711	15.3112	0.5738	1.7743	$\square\square\square$ CC (11) + $\square\square$ CCCC (70)
-	677	650	20.0402	2.8009	10.3645	β CCN (15)
-	642	617	312.3766	2.2131	9.1059	β OCC (48)
609	620	596	20.4106	2.4871	10.9601	$\square\square$ OCCC (78)
-	568	546	51.2016	0.9087	4.7646	β HOO (10) + β OCC (21) + $\square\square\square\square$ CC (16) + $\square\square\square$ CC (46)
-	560	538	120.8471	2.3639	12.7664	$\square\square$ CCOO (10) + OCOC (40)

500	536	515	941.3927	1.4190	8.3808	ν CC (60)
-	481	462	24.3424	1.2848	9.4081	ν OC (25) + β OCO (22)
-	443	426	230.2357	0.9470	8.1763	β HOO (20) + $\square\square\square\square\square\square$ (41)
-	359	345	19.4341	1.1383	14.9495	β CCO (58) + β CCO (10) + ν CC (16)
-	315	303	46.7555	0.4346	7.4162	β CCC (54)
-	306	294	129.1815	0.3048	5.5235	$\square\square\square\square$ (52)
-	264	254	3.7525	0.3922	9.5181	$\square\square\square\square$ (20) + $\square\square\square\square$ (37)
-	163	157	51.5619	0.1565	9.9844	β COO (11) + $\square\square\square\square$ (11) + $\square\square\square\square$ (47)
-	140	134	18.3088	0.0742	6.3639	$\square\square\square\square$ (12) + $\square\square\square\square$ (43) + $\square\square\square\square$ (10)
-	105	101	13.8241	0.0333	5.0672	β CCO (10) + β CCN (37)

ν - stretching, β - in plane bending, ω - out plane bending, τ - torsion

3.5 Frequency Doubling Test (SHG)

The frequency doubling (nonlinear) property of GSQ single crystal has been investigated by using the Kurtz-Perry powder technique [35]. This technique can be used to measure the Second Harmonic Generation (SHG) effective non-linearity of new materials relative to potassium Dihydrogen Phosphate (KDP). The GSQ single crystal is 1.55 times greater in second order efficiency (31 mV) when compared with the standard Potassium dihydrogen phosphate (KDP) material (20 mV) and 1.96 times greater when compared with the Urea as the reference material (61mV). From this analysis to conclude that the GSQ crystal would be an optional material in SHG device fabrications.

3.6 UV-Vis analysis

The determination of exact optical nature of the single crystal helps to identify its extended credibility for optoelectronics device and non-linear optical (NLO) applications [36]. The optically transparent single crystal is attenuated by several external, and internal crystal orientation of the system [37-38] and the physical parameters such as grain boundaries, vacancy, voids, inclusions, impurities, striations [39]. Optical absorption spectrum of the GSQ single crystal is shown in Fig. 6. The optical band gap energy value is found to be 4.62 eV is shown in fig. 7. The spectrum reveals that the transmittance of 1 mm thickness GSQ crystal is ~ 90% in entire range of spectrum. The experimental and theoretical UV-Vis graph is nearly correlated the obtained values. The sharp fall in transmittance identifies the cut-off wavelength of GSQ crystal at 286 nm (facilitated by n to π transition) and confirms the homogenous optical density of crystal. The L-Glycinium Hydrogen Squarate (GSQ) single crystal with high optical transmittance and lower cut-off wavelength is the essential devices for transmission of second and third harmonic optical signals and UV-tunable lasers etc., [40,41].

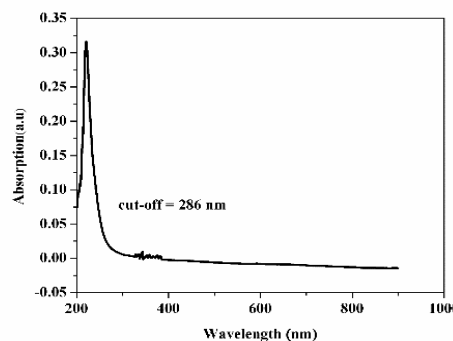


Fig. 6. UV- vis absorption spectra of GSQ crystal

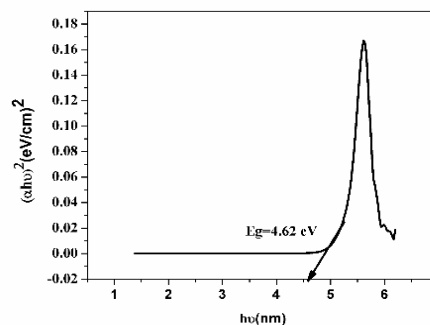


Fig. 7. UV- vis bandgap of GSQ crystal

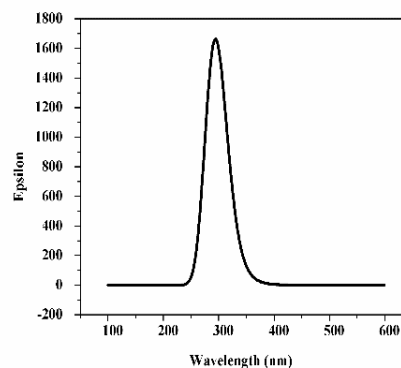


Fig.8. UV-Vis theoretical spectrum of GSQ crystal

3.7 Dielectric Studies

The dielectric constant graph shows the variation of dielectric constant for the log frequency range of 1.5-6.5 Hz is shown in Fig. 9. The dielectric constant steeply decreased with increasing frequency until 300 Hz and almost constant for the higher frequency sides. The dielectric constant at lower frequency follows linear relation with space-charge polarization. The polarisation value will be decreases then, it exhibits the decrease in the value of dielectric constant with increasing frequency [42]. The dielectric loss studies explain the ability of materials, it helps to convert the electromagnetic energy into heat energy. The variation of dielectric loss ($\tan \delta$) with frequency can be shown in Fig. 10. The dielectric loss decreases with increase of frequency. It indicates low dissipation of energy in the form of heat [43], which further confirms the quality of GSQ single crystal. The low value of dielectric constant and dielectric loss at the higher frequency suggests GSQ single crystal possess the less defects and it was suitable for NLO device applications. From fig. 11., it can be clearly seen that the value of σ_{ac} is very low up to 6 MHz and increase with increase of frequency and can be explained on the basis of frequency power law.

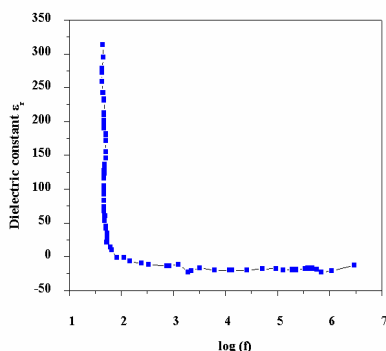


Fig. 9. Variation of dielectric constant with frequency of GSQ crystal

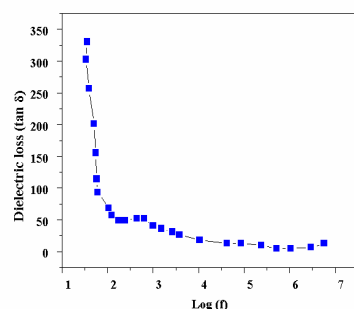


Fig. 10. Variation of dielectric constant with frequency of GSQ crystal

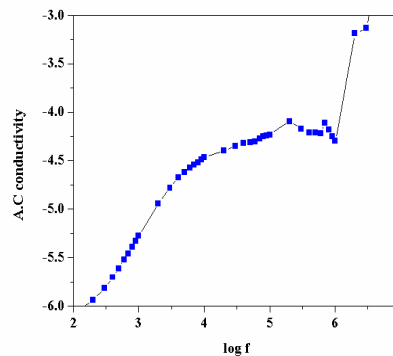


Fig. 11. Variation of A.C. conductivity with frequency of GSQ crystal

4. CONCLUSION

The thorough vibrational spectral analysis and DFT theoretical calculation were performed for GSQ single crystal. The bond lengths and bond angles (optimized geometric parameters) are theoretically determined and also, compared with the structurally similar molecules. The FT-IR spectra of the GSQ molecule are observed with the experimental and calculated vibrational wavenumbers. The theoretical results showed an acceptable general agreement with the experimental record. The frontier molecular orbitals investigation reveals the molecular energy gap. The electrical studies were also been done in the title compound. The calculated energy gap $E = 4.62$ eV, these results indicate that the GSQ single crystal might be a good candidate of NLO material. NLO efficiency was about 1.55 times and 1.96 times greater than the standard KDP material and urea respectively.

REFERENCES

- [1] J. Pecaut, J. LeFur Y, 1993 Acta Crystallogr. 49 535
- [2] S.H. Mashraqui, Kenny R S, Ghadigaonkar S G, Krishnan A, Bhattacharya M, Das P K, 2004 Opt. Mat. 27 257
- [3] L. Pauling, 1960 An Introduction to Modern Structural Chemistry Cornell University Press, (New York) 10
- [4] P. Srinivasan, T. Kanagasekaran, R. Gopalakrishnan, G. Bhagavannarayan, P. Ramasamy, 2006 Cryst. Growth Des. 6 1663
- [5] H. Bock, N. Nagel, A. Seibel, Liebigs Ann./Recueil 2006 1 2151
- [6] T. Arivazhagan, S. Siva Bala Solanki, N.P. Rajesh, 2017 Opt. Laser Technol. 88 188
- [7] M. Kurt, T.R. Serbakan, M. Ozduran, 2008 J. Mol. and Bio Mol. Spectro. 70 664
- [8] S. Senthil, S. Pari, R. John Xavier, J. Madhavan 2012 J. Optick. 123 104
- [9] D.A. Kleinman, 1962 Phys. Rev. 126 1977
- [10] C.B. Aakeroy, A.M. Beatty, M. Nievwenhuyzen, Zou M, 1988 J. Mater. Chem. 8 1385.
- [11] Edwin Sheela, D. Manimaran, I. Hubert Joe, Sherifa Rahim, V. Bena Jothy, 2015 Spectrochim. Acta A. 40 143.
- [12] N. Tagmatarchis, E. Aslanis, K. Prassides, Shinohara, 2001 Chem. Mater. 13 2374

- [13] N.I. Makela, H.R. Knuuttila, M. Linnolahti, H. Pakkanen, 2001 *J. Chem.* 1 9195.
- [14] M. Belletete, S. Beaupre, J. Bouchard, P. Blondin, M. Leclerc, G. Durocher, 2000 *J. Phys. Chem. B.* 104 9118
- [15] M. Mitsui, Y. Ohsima, 2000 *J. Phys. Chem. A* 104 8638
- [16] K. Mohana Priyadarshini, A. Chandramohan, G. Anandha Babu, P. Ramasamy, 2014 *J. Optik.* 125 1390
- [17] R.M. Silverstein, F.X. Webster, John Wiley and Sons (New York) 2005.
- [18] N.B. Colthup, L.H. Daly, S.E. Wiberley, Academic Press (New York) 1990.
- [19] G. Socrates, Wiley, Chichester, 2001.
- [20] L.J. Bellamy, Chapman and Hall, New York, Wiley, 1975
- [21] C. Karabacak Karaca, A. Atac, M. Eskici, A. Karanfil, 2012 *Spectrochim. Acta Mol. Biomol. Spectrosc.* 97 556
- [22] C. Sourisseau, P. Maraval, 25 (1994) 477-488.
- [23] A.J. Barnes, M.A. Majid, M.A. Stuckey, P. Gregory, C.V. Stead, 1985 *Spectrochim. Acta Mol. Spectros.* 41 629
- [24] G. Varsanyi, Academic Press (New York) 1969.
- [25] H. Saral, O. Ozdamar, I. Uçar, Y. Bekdemir, M. Aygün, 2016 *J. Mol. Struct.* 1103 9
- [26] B. Smith, a Systematic Approach, CRC, (Washington) DC, 1999.
- [27] N.P.G. Roeges, John Wiley and Sons Inc., (New York), 1994.
- [28] M. Arivazhagan, D. Anitha Rexalin, 2013 *Spectrochim. Acta Mol. Biomol. Spectrosc.* 104 451
- [29] S. Sudha, N. Sundaraganesan, K. Vanchinathan, K. Muthu, S.P. Meenakshisundaram, 2012 *J. Mol. Struct.* 30 191.
- [30] N.B. Colthup, L.H. Daly, S.E. Wiberley, Academic Press, (New York), 1990.
- [31] F.R. Dollish, W.G. Fateley, F.F. Bentley, Wiley-Interscience, (New York) 1974.
- [32] R.M. Silverstein, F.X. Webster, John Wiley and Sons, (New York) 2005.
- [33] I. Hubert Joe, I. Kostova, C. Ravikumar, M. Amalanathan, S.C. Pinzaru, 2009 *J. Raman Spectrosc.* 40 1033
- [34] H. Tanak, F. Ersahin, E. Agar, O. Buyukgungor, Yavuz, 2008 *j. Mol. mod.* 24 1281
- [35] S.K. Kurtz, T.T. Perry, 1968 *J. Appl. Phys.* 39 3798
- [36] V.G. Mohd Shkir, S. Alfaify, I.S. Yahia, Mohd Anis 2018 *Phys. B* 27 54217
- [37] M. Saravanan, 2016 *Opt. Mat.* 58 327
- [38] V. Pahurkar, M. Anis, M. Baig, S. Ramteke, B. Babu, G. Muley, 2016 *Optik* 127 4932
- [39] M.J. Weber Handbook of optical materials, CRC press 2002.
- [40] M. Shaikh, M. Anis, M. Shirsat, S. Hussaini, 2018 *Optik* 154 435
- [41] A. Shanthi, C. Krishnan, P. Selvarajan, 2013 *Physica Scripta.* 88 035801.
- [42] M. Anis, M. Pandian, M. Baig, P. Ramasamy, G. Muley, 2018 Taylor & Francis 22 409
- [43] L. Guilbert, J.P. Salvestrini, M.D. Fontana, and Z. Czaplá, 1998 *Phys. s. Rev. B.* 58 2523.